Composite Structures 326 (2023) 117587

Contents lists available at ScienceDirect

Composite Structures

journal homepage: www.elsevier.com/locate/compstruct

Confinement of masonry columns with FRCM: A new confined strength formulation and experimental validation

Flora Faleschini [a,*], Klajdi Toska [b,c]

[a] Department of Civil, Environmental and Architectural Engineering, University of Padova, via Francesco Marzolo 9, Padova, Italy
[b] Laboratoire de Mécanique & Matériaux du Génie Civil – L2MGC, CY Cergy Paris Université, 5 Mail Gay Lussac, 95000 Neuville-sur-Oise, France
[c] CY Institute for Advanced Studies, 1 Rue Descartes, 95000 Neuville-sur-Oise, France

ARTICLE INFO

Keywords:
Composites
Confinement
FRCM
TRM
Masonry
Strength

ABSTRACT

In this work, a wide experimental dataset about the axial behavior of masonry columns confined with Fabric Reinforced Cementitious Matrix (FRCM) jackets (also refered to as TRM - Textile Reinforced Mortar or TRCC - Textile Reinforced Cementitious Composites), that contains the results from 226 confined specimens, was collected. Data were critically analyzed with the aim of identifying the influence of the most important parameters considered within the dataset (i.e., fibers type and number of layers, masonry type and unconfined strength, mortar type and mechanical strength, the effective lateral pressure, etc.). Further, a review of the main models proposed in different Codes and in literature was carried out, which were then applied to the dataset, highlighting some discrepancies in their predictions. Thus, a new formulation for the confined strength of masonry columns was proposed, aiming to consider also some other influencing variables such as the compressive strength of the masonry blocks and that of the mortar joint. Lastly, the validity of the proposal was verified on a new set of experimental results, which were obtained by the authors testing three unconfined and confined clay brick masonry columns. Specimens were subject to monotonic axial loading under displacement control until failure, and stress and strains were monitored continuously during the test. The jacketing system was realized with one layer of glass-based FRCM (GFRCM).

1. Introduction

Design-oriented formulations should comply with the requirements of being at the same time simple, easy to be applied, and sufficiently accurate to predict the real behavior of the phenomenon under investigation. Their formulations are typically based on empirical data, collected by a single or more authors in literature; further, it is often recommendable to apply suitable partial safety coefficients (e.g., applied directly on material properties or even at the model itself), to allow them being sufficiently conservative. In the case of understanding the behavior of confined reinforced concrete (RC) or masonry elements under centered axial loading, many works proposed formulations to predict both their confined strength and ultimate strain, based on a large set of experimental campaigns. However, a general consensus indicating which formulation predicts better the above-mentioned properties is still not reached, especially when dealing with members confined by externally bonded reinforcement, i.e., fiber reinforced polymers (FRP) or fabric reinforced cementitious matrix (FRCM).

FRCM confinement has gained a lot of popularity to repair and strengthen existing masonry structures, especially when dealing with historic structures for which the intervention with FRP (that adopts organic matrix, little compatible with the substrate, and difficult to be considered reversible) results inadequate [1–2]. Even though the axial capacity of existing masonry structures is not a major issue, as they generally possess large cross-section and a sufficient compressive strength, there are cases where this problem is considered extremely important. In fact, deterioration [3], long-term phenomena [4] or even damage due to external actions (earthquakes [5] or foundation settlements [6]) may reduce the axial load bearing capacity of such structures, and this is even more evident for rubble stone columns, where the capacity is owned by the face masonry units only [7]. A typical positive feature offered by the FRCM jacketing systems relates to its failure mode, that generally favors the specimens to display a softening behavior rather than the typical abrupt failure observed when FRP is used [8–9].

According to a recent round robin test [10] carried out by many

* Corresponding author.
E-mail address: flora.faleschini@dicea.unipd.it (F. Faleschini).

https://doi.org/10.1016/j.compstruct.2023.117587
Received 28 November 2022; Received in revised form 4 September 2023; Accepted 29 September 2023
Available online 30 September 2023

authors in the Italian context, FRCM jacketing has been demonstrated to be effective both in enhancing the load bearing capacity of masonry columns, and also their ultimate axial deformation. However, the efficiency of the system depends on many variables, which are the type of fibers, the number of layers, but even the type and strength of the substrate. In fact, when poor masonry quality is used (in [10] the authors tested both tuff and clay brick masonry columns) the high expansion of the columns, occurring as a consequence of the damage applied with the axial load, cannot be carried by fiber meshes with low density. However, in [11–12] it is demonstrated that when the confinement is applied to an original column with low axial capacity, the strength increase that can be achieved by a correctly-designed FRCM jacketing system is enhanced compared to the case when the same reinforcement is applied to a column with higher mechanical properties. Other variables that were found to influence the behavior of FRCM-confined masonry are the jacket configuration (continuous or discontinuous layers [13], concentration of the overlapping zones [14]), mortar properties of the strengthening system [15–16], cross-section geometry and corner radius [17–18]. However, each author has addressed a specific problem separately, thus discussing the influence of a single parameter on a limited set of experimental results.

Recently, several authors recognized the necessity to provide a suitable model to evaluate the bearing capacity of confined masonry columns, as a result of an overall discrepancy of the predictions obtained when adopting current Codes or literature formulations [19–21]. Particularly, Napoli and Realfonzo [19] highlighted the importance of calibrating coefficients for the different FRCM systems that can be applied, however facing the problem of the few data availability to assess the strain efficiency as a result of lack of fibers strain monitoring in the existing experimental campaigns. The same conclusion was achieved in [22], where authors highlighted the importance of bond between the fibers and mortar in the whole ability of the composite to exploit its strength, and thus to apply the lateral pressure to the confined masonry core. However, the application of design-oriented models requires simplified approaches, with a limited number of influencing parameters whose contribution should be supported by reliable experimental data: as a result, at least until now, a single proposal for each FRCM type seems inadequate to the scope.

In this work, to contribute to the existing knowledge in the field, an extensive dataset of experimental results of confined masonry columns was collected from literature. Compared to others recently published, e.g., [19], the present one is slightly broader and contains 226 records. The influence of the main parameters varying in the dataset is analyzed in Section 2. Instead, Section 3 reviews the current available models for predicting the strength of confined masonry columns. All the formulations were then applied to the collected dataset and statistical indicators that show the goodness of fitting of each proposal are calculated. Section 4 proposes a new design-oriented formulation for assessing the confined strength of masonry columns, which has been calibrated on the collected dataset, and differs from the ones already present in literature from the initial parameters to be considered. Lastly, Section 5 reports the results of an experimental campaign carried out by the authors on six clay-brick masonry columns; three of them were used as unconfined reference samples, and three were confined with a single layer of GFRCM. The new analytical formulation is applied to this new set of results, highlighting its good prediction performance on a different dataset from the original one. Finally, the Conclusion section is provided.

2. Experimental dataset

The dataset comprises 226 confined masonry columns with squared or rectangular cross-section, is based on the review of 24 published works [1–2,5,10–12,14,17–18,23–37] and it is provided in the Annex. For each specimen, the following parameters were collected: cross section geometry, width b, height h, length of the diagonal D, corner radius r_c; specimen height L; compressive strength of the brick or stone f_{bc}; compressive strength of the mortar joint f_j; overall thickness of the FRCM jacket t_{mat}; compressive strength of the inorganic matrix $f_{c,mat}$; type of fiber F; number of FRCM layers n_f; equivalent thickness of the single layer of the fiber sheet t_f; elastic modulus of dry strengthening sheet E_f; matrix reinforcement ratio ρ_f; ultimate strain of dry strengthening sheet ε_{fu}; unconfined compressive strength of the masonry column f_{c0}; confined compressive strength of the masonry column f_{cc}. Other variables of interest, such as the masonry mass density (g_m), were not available for all the analyzed specimens, and thus were not compiled.

Most of the specimens of the dataset have a squared cross-section (178 over 226) and only 48 have a rectangular section. The main types of masonry units adopted are new clay-brick or calcareous-rocks, but there are cases where also blocks were extracted from existing buildings [28]. Different types of fibers were adopted: 45 specimens were strengthened with basalt fibers, 60 with glass, 71 with steel, 36 with carbon and lastly 14 with polybenzobisoxazole (PBO). The great majority of the specimens failed after the development of wide cracks that concentrated at the section edges, and in some cases in the region of the overlapping length. In both the situations, fibers achieved the ultimate strain after some slippage phenomena [19,31,33]. To sum up the range of variations of the collected data for each specimen, the main features of the distribution for each quantitative parameter characterizing the samples collected in the dataset are shown in Table 1. There, the minimum, maximum, average, the three quartiles (25% Q1, 50% Q2 and 75% Q3) and the interquartile range (IQR = Q3-Q1) are listed. It can be noted that for some parameters, the range of the variation is quite limited, e.g., for the equivalent thickness of the single layer of the fiber sheet, the compressive strength of the inorganic matrix and for the number of layers, even if some outliers are clearly present (note that n_f varies from 1 until 7, but the upper quartile is still 2). For other parameters, such as the cross-section diameter, the compressive strength of the joint mortar and particularly the elastic properties of the fibers, the variations are much higher, as clearly visible from the high values assumed by the IQR indicator. This analysis highlights how very often the same (or very similar) organic matrix was used by different authors, even if different fiber types were adopted.

In terms of average compressive strength gain, the ratio between f_{cc}/f_{c0} is higher for the specimens retrofitted with FRCM systems based on PBO fibers, followed by those strengthened with steel, carbon, glass and basalt fibers (Table 2). However, the numerousness of the samples for each category varies significantly, making less reliable the results obtained for the columns strengthened with PBO-FRCM, compared to the other systems.

Concerning the influence of the main confinement parameters on f_{cc}/f_{c0}, the following parameters were analyzed: $t_{mat} \cdot f_{c,mat}$; $\rho_{mat} \cdot f_{c,mat}$; $t_f \cdot E_f$; $\rho_f \cdot E_f$; $2r_c/max(b; h)$; k_h; f_l; $f_l \cdot r_c$; $f_l \cdot 2r_c/max(b; h)$; $f_l \cdot k_h$; f_l/f_{c0}; $f_l \cdot k_h/f_{c0}$. Recall the general expressions for circular and square/rectangular cross-sections:

$$\rho_{mat} = 4t_{mat}/D \text{ and } \rho_{mat} = 4t_{mat}/\sqrt{b^2 + h^2} \quad (1)$$

$$\rho_f = 4n_f t_f/D \text{ and } \rho_f = 4n_f t_f/\sqrt{b^2 + h^2} \quad (2)$$

where ρ_{mat}, similarly to ρ_f, is the matrix reinforcement ratio, k_h is the horizontal efficiency coefficient (equal to 1 in case of circular cross-section, only), that can be evaluated as the effectively confined masonry area over the cross-section area:

$$k_h = 1 - \frac{(b - 2r_c)^2 + (h - 2r_c)^2}{3bh} \quad (3)$$

Instead, f_l is the lateral pressure exerted by the FRCM jacket to the confined masonry column, and it can be generally evaluated (without assuming any reduction coefficients applied to the ultimate strain capacity of the fibers) as:

Table 1
Descriptive statistics of the specimens' features collected in the dataset.

	D (mm)	r_c (mm)	f_{bc} (MPa)	f_j (MPa)	t_{mat} (mm)	$f_{c,mat}$ (MPa)	n (-)	t_f (mm)	E_f (GPa)	ρ_f (-)
Min	142.84	0	5.26	0.55	6	0.55	1	0.012	59.8	0.022
Max	725.60	38.1	95.4	16.90	24	58.1	7	0.250	240.0	0.574
Ave	384.19	18.47	24.04	5.83	11.85	21.92	1.80	0.077	146.4	0.137
Q1	353.55	12	11	3.54	10	10.37	1	0.056	71.0	0.072
Q2	353.55	20	19.33	4.35	10	15	1	0.078	193.7	0.096
Q3	441.02	20	26.2	6.98	15	35	2	0.085	205.0	0.192
IQR	87.47	8	15.2	3.44	5	21.92	1	0.029	134.0	0.120

Table 2
Influence of fiber types on the strength gain according to the experimental results collected in the dataset.

Fiber type	Number of specimens	f_{cc}/f_{c0}
Basalt (B)	45	1.24
Carbon (C)	36	1.38
Glass (G)	60	1.35
PBO	14	2.27
Steel (S)	71	1.47

$$f_l = \frac{2n_f t_f E_f \varepsilon_{fu}}{D} = \frac{1}{2}\rho_f E_f \varepsilon_{fu} \tag{4}$$

Simple linear regression analyses were carried out aiming at obtaining statistical correlations between the variable to be predicted (i.e., the strength gain) and each predictor. Fig. 1 shows the results, where for each relation, the root mean square error (*RMSE*) and the determination index (R^2) are reported: the highest is the *RMSE* value, the highest is the dispersion of the prediction; the highest is the R^2 value, the highest is the correlation between the two variables. A low statistical dependency of the strength gain can be identified on the analyzed parameters. Such result depends on the high variability of the results, as demonstrated by the great dispersion of the predictions (see the *RMSE* value, always higher than 0.2). However, the R^2 values are significantly

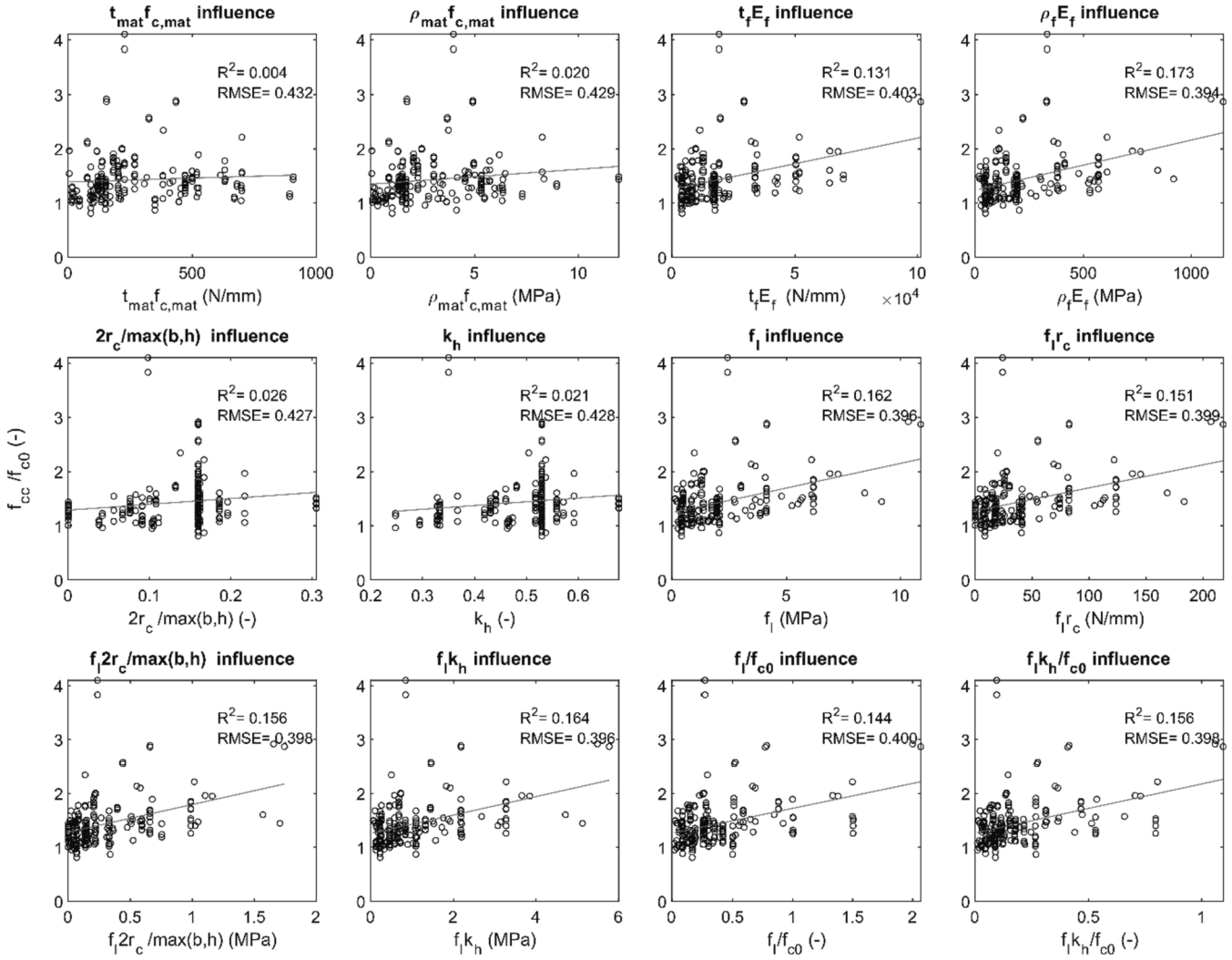

Fig. 1. Main influencing parameters.

improved in some cases: for instance, the lateral pressure exerted by the FRCM jacket shows a non-negligible influence on the strength gain, especially when combined with the horizontal efficiency coefficient ($f_l \cdot k_h$), or with the geometrical features of the cross-section. Accordingly, the parameters displaying the highest R^2 should be considered into a predicting model for the masonry confined compressive strength estimation.

3. Existing models

Current available literature has mainly focused in proposing predictive models for assessing the confined compressive strength of masonry by means of FRP jacketing techniques, and only seldom analytical formulations were proposed for FRCM-confined members. Table 3 collects the main analytical formulations proposed by codes, guidelines and other authors, in case of continuous external reinforcement applied to a masonry unit. As it can be quickly observed, most of the variables analyzed in Section 2 are present in the formulations. The typical expression of current models is based on quantifying the equivalent uniform confining pressure exerted by the reinforcing jacket to the masonry core. To this scope, the lateral pressure exerted by the FRCM jacket is generally computed with Eq. (4), and then is modified considering the cross-section geometry via the horizontal efficiency coefficient k_h. Such coefficient is computed differently among the

Table 3
Existing predicting formulations for f_{cc} of masonry-confined columns with FRCM.

Source	Model	Notes
CNR DT 215 [38]	$f_{cc} = f_{c0}\left[1 + \frac{g_m}{1000}\left(\frac{f_{l,eff}}{f_{c0}}\right)^{0.5}\right]$	$f_{l,eff} = k_h f_l$ $k_h = 1 - \frac{(b-2r_c)^2 + (h-2r_c)^2}{3bh}$ $f_l = \frac{2n_f t_f E_f \varepsilon_{u,rid}}{D}$ $\varepsilon_{u,rid} = \min(\eta_A k_{mat} \varepsilon_{fu}/\gamma_m; 0.004)$ η_A is the environmental coefficient (to be set equal to 0.9 for inner exposition) γ_m is the safety partial coefficient (to be set equal to 1.5) $k_{mat} = 1.81(\rho_{mat}\frac{f_{cmat}}{f_{c0}})^2 \leq 1$
ACI 549.4R [39]	$f_{cc} = f_{c0}\left(1 + 3.10\frac{f_{l,eff}}{f_{c0}}\right)$	$f_{l,eff} = k_h f_l$ $k_h = \left(\frac{b}{h}\right)^2\left[1 - \frac{\frac{h}{b}(b-2r_c)^2 + \frac{b}{h}(h-2r_c)^2}{3bh}\right]$ $f_l = \frac{\rho_f E_f \varepsilon_{fu}}{2}$
Cascardi et al. [40]	$f_{cc} = f_{c0}\left[1 + k\left(\frac{f_{l,eff}}{f_{c0}}\right)^{0.5}\right]$	$f_{l,eff} = k_h f_l$ $k_h = 1 - \frac{(b-2r_c)^2 + (h-2r_c)^2}{3bh}$ $f_l = \frac{\rho_f E_f \varepsilon_{fu}}{2}$ $k = 6\rho_{mat} f_{cmat}/f_{c0}$
Jing et al. [20]	$f_{cc} = f_{c0}\left[1 + 0.65\left(\frac{f_{l,eff}}{f_{c0}}\right)^{0.19}\right]$	$f_{l,eff} = k_h f_l$ $k_h = 1 - \frac{(b-2r_c)^2 + (h-2r_c)^2}{3bh}$ $f_l = \frac{\rho_f E_f \varepsilon_{fu}}{2}$
Krevaikas -linear [17]	$f_{cc} = f_{c0}$ *if* $\frac{f_{lu}}{f_{c0}} < 0.09$ $f_{cc} = f_{c0}\left[0.88 + 1.324\frac{f_{lu}}{f_{c0}}\right]$ *if* $f_{l,eff}/f_{c0} \geq 0.09$	$f_{lu} = k_h\frac{(b+h)}{bh} t_f E_f \varepsilon_{fu}$
Krevaikas –non linear [17]	$f_{cc} = f_{c0}\left[1 + 1.65\left(\frac{f_{lu}}{f_{c0}}\right)^{1.84}\right]$	$f_{lu} = k_h\frac{(b+h)}{bh} t_f E_f \varepsilon_{fu}$
Koutas and Bournas [36]	$f_{cc} = f_{c0}\left[1 + 2.836\left(\frac{f_{lu}}{f_{c0}}\right)^{\alpha}\right]$	α is 1 for carbon, glass, basalt textiles $f_{lu} = k_h f_l$
Ameli et al. 1 [22]	$f_{cc} = f_{c0}\left[1 + 82.13k_H\left(\frac{n_f t_f}{D}\right)^{0.74}\left(\frac{E_f f_{tmat}}{f_{c0} E_{mat}}\right)\right]$	f_{tmat} is the direct tensile strength of the matrix E_{mat} is the elastic modulus of the matrix $k_h = 1 - \frac{(b-2r_c)^2 + (h-2r_c)^2}{3bh}$
Ameli et al. 2 [22]	$f_{cc} = f_{c0}\left[1 + 12.72k_H\left(\frac{n_f t_f}{D}\right)^{0.5}\left(\frac{E_f f_{tmat}}{f_{c0} E_{mat}}\right)\right]$	f_{tmat} is the direct tensile strength of the matrix E_{mat} is the elastic modulus of the matrix $k_h = 1 - \frac{(b-2r_c)^2 + (h-2r_c)^2}{3bh}$
Napoli and Realfonzo 1 [19]	$f_{cc} = f_{c0}\left[1 + 0.40\left(\frac{g_m}{1000}\right)^2\left(\frac{f_{l,eff}}{f_{c0}}\right)^{0.75}\right]$	$f_{l,eff} = k_h k_{mat} f_l$ $k_h = 1 - \frac{(b-2r_c)^2 + (h-2r_c)^2}{3bh}$ $f_l = \frac{2n_f t_f E_f \varepsilon_{fu}}{D}$ $k_{mat} = 1$
Napoli and Realfonzo 2 [19]	$f_{cc} = f_{c0}\left[1 + 1.10\left(\frac{f_{l,eff}}{f_{c0}}\right)^{2/3}\right]$	$f_{l,eff} = k_h k_{mat} f_l$ $k_h = 1 - \frac{(b-2r_c)^2 + (h-2r_c)^2}{3bh}$ $f_l = \frac{2n_f t_f E_f \varepsilon_{fu}}{D}$ $k_{mat} = 0.90$

models, even if the general expression is provided in Eq. (3) according to numerous evidences from experimental tests. The lateral pressure f_l can be further reduced to consider the premature failure of the FRCM jacket, as a consequence of masonry buckling phenomena or stress concentration at the section edges, or the low exploitation of the fibers inside the system due to fiber slippage inside the matrix. Some authors recommended to reduce the ultimate tensile strength of the fibers by 15% [21], in other cases a limitation to the ultimate strain capacity of the system is imposed [38]. Lastly, each model is calibrated on a series of experimental results, thus different coefficients are adopted in the formulations, resulting in some cases in linear and in others in non-linear functions of the effective lateral pressure over the unconfined compressive strength ratio.

The analyzed models were applied to the final dataset collected in this work, to evaluate their performance to predict the experimental results. For those expressions where g_m is present, this parameter was assumed equal to 1700 kg/m^3. Further, for the formulations provided by Ameli et al. [22], where both the direct tensile strength and the elastic modulus of the mortars are included, these variables were calculated based on the relations for concrete available in the Eurocode 2 [41]:

$$f_{tmat} = 0.3 f_{ck}^{\frac{2}{3}} \tag{5}$$

$$E_{cm} = 22000 (f_{cm}/10)^{0.3} \tag{6}$$

assuming a unitary partial safety coefficient applied to f_{ck}, and considering that the maximum compressive strength of the mortar in the dataset does not exceed 60 MPa. The prediction precision of the analyzed existing confinement models is shown in Fig. 2, while the main statistical parameters are summarized in Table 4. Particularly, *AVE.* (i.e., the mean ratio $f_{cc,theo}/f_{cc,exp}$), *ST.DEV.* (i.e., the standard deviation of the ratio $f_{cc,theo}/f_{cc,exp}$), R^2 and *RMSE* accuracy indicators were calculated. The indicators connected with the best model performance are indicated in bold in Table 4.

Some considerations about the accuracy of the predictions are listed below:

- CNR DT-215 [38] shows a relatively high coefficient of determination ($R^2 = 0.73$) and is characterized by low scattering results. The standard deviation is one of the lowest compared to the other

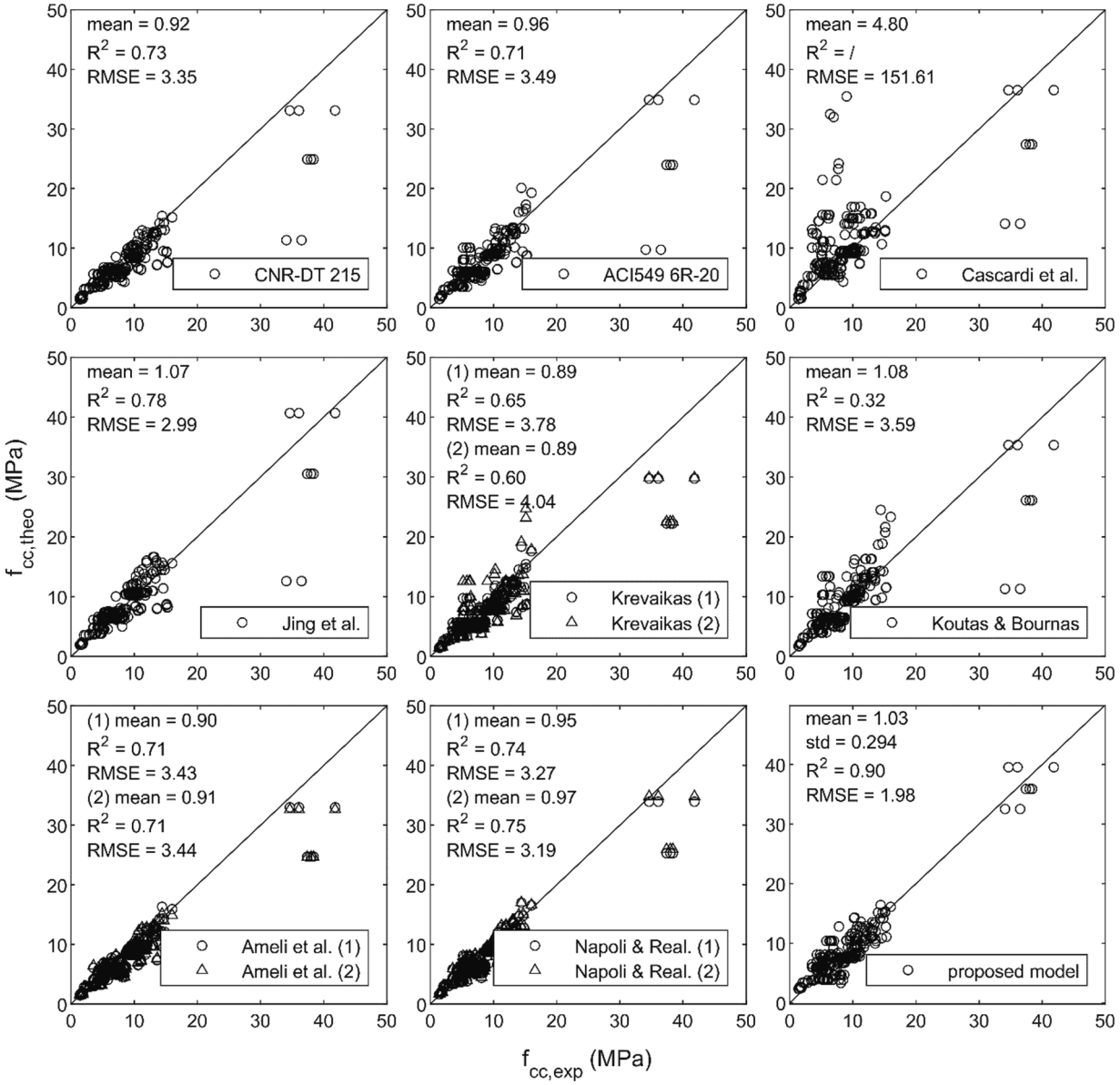

Fig. 2. Assessment of existing masonry FRCM-confinement models.

Table 4
Accuracy indicators for the analyzed and the proposed predicting models.

Model	*AVE*	*ST. DEV.*	R^2	*RMSE*
This proposal	**1.031**	0.294	**0.904**	**1.983**
CNR DT 215 [38]	0.922	0.193	0.728	3.354
ACI 549.4R [39]	0.962	0.240	0.705	3.490
Cascardi et al. [40]	4.796	10.680	-	-
Jing et al. [20]	1.066	0.219	0.783	2.994
Krevaikas - linear [17]	0.892	0.225	0.655	3.778
Krevaikas - nonlinear [17]	0.890	0.279	0.605	4.041
Koutas and Bournas [36]	1.085	0.323	0.689	3.586
Ameli et al. 1 [22]	0.896	**0.187**	0.715	3.432
Ameli et al. 2 [22]	0.906	0.191	0.713	3.444
Napoli and Realfonzo 1 [19]	0.948	0.200	0.741	3.273
Napoli and Realfonzo 2 [19]	0.966	0.201	0.755	3.185

analyzed models (0.19), while the *RMSE* is in the average of the results obtained for the other models. The model is conservative as the mean $f_{cc,theo}/f_{cc,exp}$ values is about 0.92. In this case, it should be recalled that the assumption made on g_m might have influenced the results.

- ACI549-6R-20 [39] performs well in terms of $f_{cc,theo}/f_{cc,exp}$, which is about 0.96. The standard deviation is higher than the previous model (about 0.24), while the R^2 and *RMSE* are about 0.7 and 3.5 respectively.
- The model proposed by Cascardi et al. [40] does not consider strain limitations for the confinement systems. This causes the model to highly overestimate some specimens' results, and therefore to have statistical parameters out of the range of those observed for the other models.
- The model proposed by Jing et al. [20] has the highest coefficient of determination and the lowest *RMSE* values, being 0.78 and 2.99 respectively. The model however tends to overestimate the strength enhancement of confined columns by nearly 7%, this being unconservative for a design-oriented model purpose.
- Krevaikas [17] proposed two relations, one linear and one nonlinear, for masonry FRCM confinement. Both models are conservative with a mean $f_{cc,theo}/f_{cc,exp}$ of 0.89, however, the linear one performs better in terms of standard deviation, R^2 and *RMSE*.
- Similar to Jing et al. [20], the model by Koutas and Bournas [36] is unconservative, and it performs slightly worse than [20] for all the other indicators.
- Very recently, Ameli et al. [22] proposed two models for the confined compressive strength of masonry columns. The models, a part from the fiber characteristics, considers also the compressive strength and the elastic modulus of the matrix. The predictions show a very low scatter but the models are highly conservative ($f_{cc,theo}/f_{cc,exp} = 0.9$) and do not perform better than other existing ones, both in terms of R^2 and *RMSE*. It is worth recalling that, in this case, the assumptions made to calculate the mortar tensile strength and elastic modulus, which are data typically not available from the experimental tests collected in the dataset, might have influenced the result. Further, according the authors of the present work, a design-oriented model should avoid to include too many parameters which are difficult to be characterized, such as in the case of [22]: in the practice, mortar properties are often characterized via flexural and compressive strength test, and only seldom the elastic modulus is analyzed.
- In terms of mean $f_{cc,theo}/f_{cc,exp}$, the models by Napoli and Realfonzo [19] are the best performing ones, with mean values of about 0.95 and 0.97 respectively. The R^2 and *RMSE* are second only to the Jing et al. [20] model, while the standard deviation is relatively low (about 0.2 for both models). Also in this case, it is worth recalling that the assumption on the masonry mass density might have influenced the result.

4. New confined strength formulation proposal

When dealing with confinement technique, apart from the characteristics of the confinement system itself, a key parameter is the initial unconfined strength of the analyzed material. Masonry is a heterogeneous material, formed by the continuous overlapping of bricks and mortar layers, and the variation of the characteristics of one of the elements may cause significant variations in the compressive strength of the whole masonry unit. For the existing structures, compressive strength is generally unknown, and its determination requires invasive and expensive in situ or laboratory tests. Even when these tests are carried out to improve the knowledge level, they are few and concern limited portions of the structure. Therefore, sometimes they fail to detect differences in the characteristics of the masonry or even in the different level of deterioration that may be present, which often affects the mortar joint only, and thus its strength.

To overcome this problem and to give a valid alternative to the various masonry confinement models already present in the literature, the present paper proposes a new formulation dependent on the compressive strength of the mortar and bricks that constitute the masonry.

Most of confined strength formulations, independently of the confinement system or the confined material are based on the generic equation:

$$f_{cc} = f_{c0}\left[1 + k\left(\frac{f_{l,eff}}{f_{c0}}\right)^{a}\right] \tag{7}$$

where:

f_{c0} is the unconfined strength, f_{cc} is the confined strength, $f_{l,eff}$ is the effective confinement pressure and lastly, k and α are equation coefficients, generally obtained via regression analyses on a dataset of experimental measures.

Instead, masonry compressive strength depends on the brick (f_{bc}) and mortar joint (f_j) strength and the general relationship used to compute this value is:

$$f_m^{'} = K f_{bc}^{\alpha} f_j^{\beta} \tag{8}$$

For sake of clarity, f_{c0} will be used to indicate the unconfined strength based on experimental results while $f_m^{'}$ for the unconfined masonry compressive strength estimated using Eq. (8), based on the brick and mortar joint strength. It should be remarked that this work does not evaluate the prediction accuracy of the masonry compressive strength models, but uses it only as a basis for the confined strength formulation.

To express the confined strength separately as a function of the compressive strength of the brick (f_b) and mortar (f_j), we can rewrite Eq. (7) using Eq. (8) as:

$$f_{cc} = K f_{bc}^{\alpha} f_j^{\beta}\left[1 + k\left(\frac{f_{l,eff}}{K f_{bc}^{\alpha} f_j^{\beta}}\right)^{a}\right] \tag{9}$$

Different coefficients were calibrated and proposed based on the above general Eq. (7) to compute the strength of masonry ($f_m^{'}$). Initially three $f_m^{'}$ formulations were considered for the calibration of the general FRCM-confinement formulation (eq. (9), based on the models proposed by Dayaratnam [42], Kaushik et al. [43] and Eurocode 6 [44]. The analysis showed that the formulation of Dayaratnam [42], shown in equation (10), gave the best results and was therefore considered for the present proposal.

$$f_m^{'} = 0.275 f_{bc}^{0.5} f_j^{0.5} \tag{10}$$

Based on the above Eqs. (7)–(10), the following FRCM confined strength formulation for masonry columns is proposed:

$$f_{cc} = 0.275 f_{bc}^{0.5} f_j^{0.5} \left[1 + 10.2 \left(\frac{f_{l,eff}}{0.275 f_{bc}^{0.5} f_j^{0.5}} \right)^{0.225} \right] \quad (11)$$

where:

$$f_{l,eff} = k_h k_f k_t \frac{(b+h)}{bh} f_l \quad (12)$$

$$f_l = \frac{2 n_f t_f E_f \varepsilon_f}{D} \quad (13)$$

$$\varepsilon_f = min(\varepsilon_{fu}, 0.012) \quad (14)$$

k_h, k_f, k_t, are coefficients regarding respectively, shape, fiber material and fiber thickness and can be considered as follows:

$$k_h = \begin{cases} 1, & circular\ sections \\ 1 - \dfrac{(b-2r_c)^2 + (h-2r_c)^2}{3bh}, & rectangular\ sections \end{cases} \quad (15)$$

$$k_f = \begin{cases} 0.30, & carbon,\ glass\ and\ basalt \\ 0.75, & PBO\ and\ steel \end{cases} \quad (16)$$

$$k_t = \frac{t_{ref} - t_f}{t_{ref}} \qquad \left(where\ t_{ref} = 1\ mm \right) \quad (17)$$

and all the other parameters were already defined in Section 2.

Compared to the other formulations, this proposal presents novelties also in the calculation of the effective confinement pressure ($f_{l,eff}$). In addition to the well-known cross-section shape coefficient (k_h), two further coefficients are introduced: one for the fiber material (k_f), and one for fiber thickness (k_t). k_f depends on the fabric efficiency when used in FRCM systems and is taken from experimental results on concrete confinement [45–48]. Based on the lateral strains measured directly on the fibers inside the confining jackets in [45], a fiber coefficient (k_f) of 0.3 is proposed for dry carbon and glass fibers. PBO and steel fibers are generally more efficient in FRCM systems than other fiber materials. Colajanni et al. [48] reported k_f values of 0.51 for specimens with 100 mm overlapping length and 0.75 for specimens with 250 mm overlapping length. Given the limitations on overlapping length provided by standards and guidelines for FRCM design [38] a $k_f = 0.75$ is suggested for PBO and steel fibers. Instead, k_t takes into the account the reduced efficiency of the FRCM systems when fabrics with high equivalent thickness (t_f) are embedded in the matrix. The thickness of each single layer for fabrics of FRCM systems are generally low (about 0.05 mm). However, increasing the fabric weight does not lead to a linear increase in strength enhancement of the confined element, because the composite is not be able to fully exploit all of the amount of reinforcement embedded in the matrix. For this reason, a simple reduction coefficient that considers the equivalent thickness of the fabric is introduced (Eq. (17)).

It was noted that the ultimate fiber strain (ε_{fu}) has a negligible effect on the confinement effectiveness as the system never fully exploits the deformation capacity of the fiber, as diffusely discussed in [22], mainly due to bond-related aspects. It was therefore preferred to introduce a limitation to the maximum axial strain of the fibers considered in the calculation of the lateral confining pressure (f_l) to 0.012 in accordance with [39]. Similar considerations were made by other authors observing the failure mode of masonry columns, resulting in a limitation of the deformation capacity [38] or in the introduction of other parameters [22].

The accuracy of this formulation is compared to that of the other ones reported in Table 4, too: for three over the four indicators, the proposal made in this work is characterized by the best performance (*AVE*, R^2, *RMSE*). It is worth citing, however, that the formulation is calibrated on the present dataset thus, for a proper assessment of its accuracy, it is necessary to apply it to a new set of experimental data, which is the objective of the next Section 5.

5. Experimental validation

5.1. Materials, strengthening protocol and test setup

To evaluate the goodness of the proposed formulation on a new set of data, an experimental campaign was carried out aimed at analyzing the behavior of three unconfined (labelled with the nomenclature "NC") and three confined small-scale masonry columns (labelled with the letter "C"). All the specimens were made with clay brick masonry with good mechanical properties, whereas the joints were made with a low-quality mortar, that is as a natural hydraulic lime one. The material properties used in the six specimens are listed in Table 5. Particularly, the compressive strength f_{bc} for the bricks, the compressive and flexural strength f_j and $f_{j,f}$ for the mortar joint are based on experimental tests carried out on at least three samples for each analyzed property, following the EN standard methods.

To realize the specimens, 18 bricks per each column were used: first, they were immersed in water for 24 h at 20 °C, to ensure a proper hydration; after this period the columns were casted, following the layout shown in Fig. 3. All the columns have the same geometry: square cross section 250 × 250 mm ($b \times h$), length of the diagonal 353.6 mm (D), column height 615 mm (L), the thickness of the mortar joint is 15 mm, whereas the height of single bricks is 55 mm. The external surface was rounded with a corner radius of 20 mm, this being the minimum prescription recommended by [38]. Concerning the mortar, which is a premixed compound of natural sand and lime, it was hydrated at an average water/solid ratio of 0.11, according to the producer recommendation, and was mixed for 120 s before its application. Some differences in the water addition were made during the realization of the columns, to allow achieving slight differences in the mortar joint strength, and thus obtaining a certain variability in the values assumed by this parameter. After columns realization, they were covered with humid tissues and plastic bags for 7 days, and then left curing for other 21 days until the moment of the strengthening.

The FRCM composite is made by a lime-based mortar and glass fibers (GFRCM system). Both these two components are provided by the same producer. The repair mortar is characterized by a higher strength than the one used for casting the columns, and is hydrated at water/solid ratio of 0.20. The glass fiber is a dry, open mesh textile, made of E-glass fiber bundles epoxy-coated, classified as alkali-resistant by the producer. For the GFCRM, the compressive and flexural strength $f_{c,mat}$ and $f_{mat,f}$ for

Table 5
Specimens characteristics.

	f_{bc} (MPa)	f_j (MPa)	$f_{j,f}$ (MPa)	$f_{c,mat}$ (MPa)	$f_{mat,f}$ (MPa)	n (-)	t_f (mm)	f_t (MPa)	E_f (GPa)
NC1	42.51	3.84	1.69	–	–	–	–		–
NC2	42.51	3.40	1.60	–	–	–	–		–
NC3	42.51	1.84	1.01	–	–	–	–		–
C1	42.51	2.45	1.24	19.38	4.40	1	0.05	2000	70.0
C2	42.51	1.51	0.49	21.80	5.08	1	0.05	2000	70.0
C3	42.51	3.49	1.48	18.10	4.59	1	0.05	2000	70.0

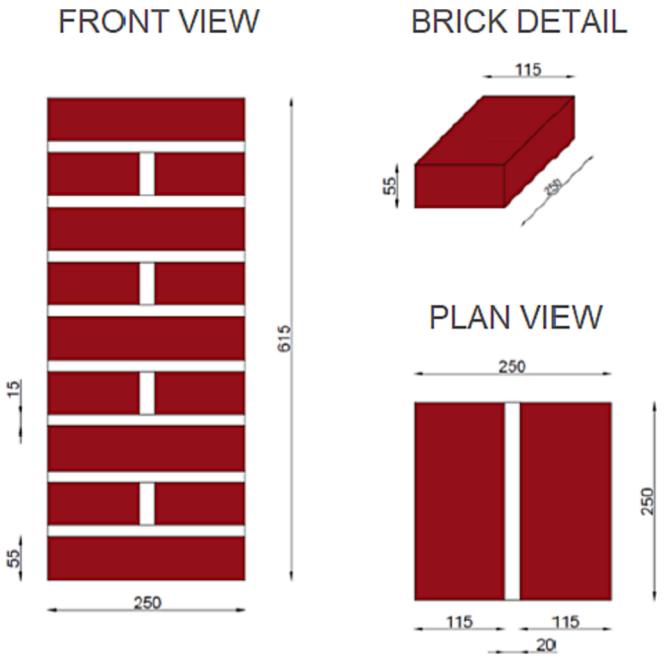

Fig. 3. Specimens geometry and bricks layout. Dimensions in (mm).

repair mortar, the number of layers n, the equivalent thickness of the single layer of the fiber sheet t_f, fiber ultimate tensile strength f_t, fiber elastic modulus E_f and lastly, the matrix reinforcement ratio ρ_f are listed in Table 5, too. Mortar material properties are based on experimental tests following the EN standard methods, carried out at least on three samples for each material property; instead, fiber properties are provided by the manufacturer.

The strengthening protocol requires a preliminary cleaning of the column surface from any powder residue; than a first layer of about 5 mm of repair mortar is applied, which is followed by the application of the glass textile, that is maintained gently in tension by hands during the jacketing operation; lastly, a finishing layer of repair mortar is applied again, with the same thickness of the first one. It should be recalled that the overlapping length was fixed for all the specimens and equal to 250 mm, i.e., one side of the column. Once the intervention was concluded, the specimens were covered with humid tissues and a plastic film to maintain the humidity for 28 days. After this curing, both the top and bottom of the columns were strengthened with one layer of carbon FRP. Fig. 4 shows the different steps of the strengthening operations.

The monotonic centered axial loading tests were carried out after 28 days from the strengthening operations for both the unconfined and confined specimens, under a displacement control mode at 0.3 mm/min. The load is continuously acquired by a pressure transducer, together with the axial strains, measured with a set of different instrumentations. Loading was stopped when the load peak drops at least by 20%, which is also considered as the failure condition of the columns. To record the axial strains, two mechanical strain gages (mSGs) were mounted on the

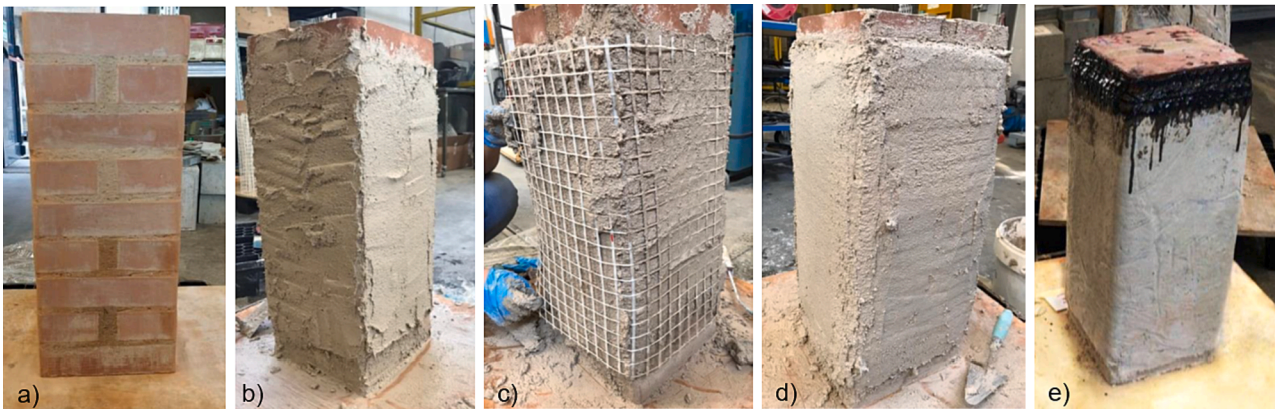

Fig. 4. Strengthening operations: a) NC column; b) first mortar layer; c) glass fiber net; d) finishing mortar layer; e) FRP top layer application.

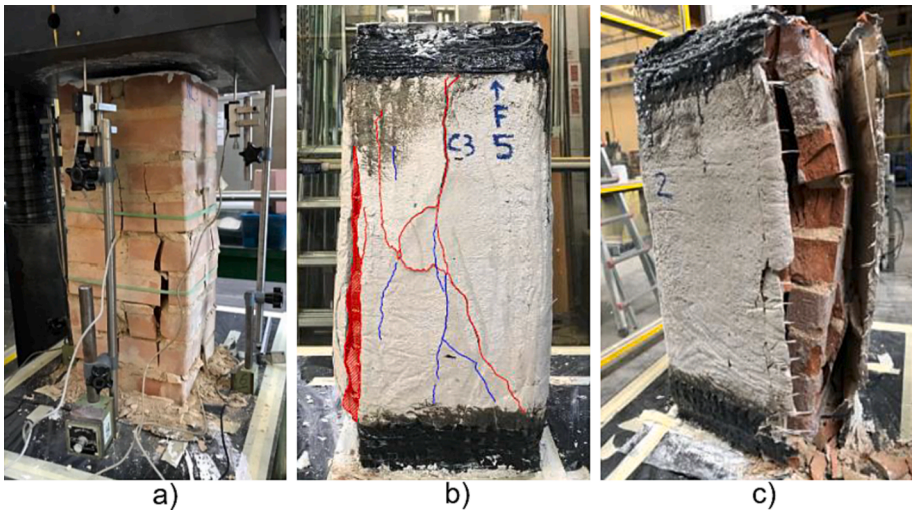

Fig. 5. Failure mode of the: a) NC3 column; b) C3 column; c) detail of the C3 column with fibers breakage and bricks crushing.

Table 6
Experimental results.

	f_{c0} (MPa)	ε_{c0} (%)	$\varepsilon_{c,u}$ (%)	f_{cc} (MPa)	ε_{cc} (%)	$\varepsilon_{cc,u}$ (%)
NC1	7.85	1.14	1.51	–	–	–
NC2	7.28	0.92	1.35	–	–	–
NC3	4.75	1.21	1.98	–	–	–
C1	–	–	–	6.96	1.49	2.85
C2	–	–	–	5.85	0.72	1.15
C3	–	–	–	7.61	1.40	2.10

external surface of the specimen in two opposite sides of the column at the mid-height (gauge length of 250 mm). Further, four linear voltage displacement transducers (LVDTs), one per each side of the column, were used to monitor the real displacement between the two rigid plates of the loading frame (the gauge length is the entire height of the column). On two columns, fiber strains were monitored during the loading history using two electrical strain gages (eSGs) directly installed in the glass mesh at mid-height of the column and in specular positions. This setup was already applied by the authors to test reinforced concrete columns strengthened with FRCM, being particularly satisfactorily to register both the pre- and post-peak strains [49–50].

5.2. Experimental results and validation

The failure mode of the unconfined columns is brittle and it shows the development of wide vertical cracks, that started from a load of about 50% of the maximum attained one, and which width increased until the peak. The cracks intercept both the vertical mortar joints and the bricks, that in some case reach a complete crushing (Fig. 5a). Instead, for the confined specimens, the failure was achieved with the development of one main vertical crack at a corner (Fig. 5b), where the stress concentration leads to the fibers breakage. After the test, in fact, it was possible to look inside the crack and detect clearly fibers tensile failure. The masonry inside the FRCM jacket appeared, after the test, severely damaged, with an extensive crushing of the clay bricks (Fig. 5c). Other minor vertical cracks formed in the jacketing system, which however were characterized by a reduced thickness compared to the principal at the section edge. No relevant signs of fibers slipping were observed.

Results are then discussed in terms of stress–strain curves until failure. The analyzed parameters are, for the unconfined columns: the peak axial strength (f_{co}), peak and ultimate axial strains (ε_{co} and $\varepsilon_{co,u}$, respectively). For the confined specimens, instead: the peak confined compressive axial strength (f_{cc}), peak and ultimate axial strains (ε_{cc} and $\varepsilon_{cc,u}$, respectively). Axial strains were computed using the mean values of the four LVDTs installed at each side of the column. Table 6 summarizes the results, whereas Fig. 6 shows the axial stress–strain and axial stress-fiber strain curves.

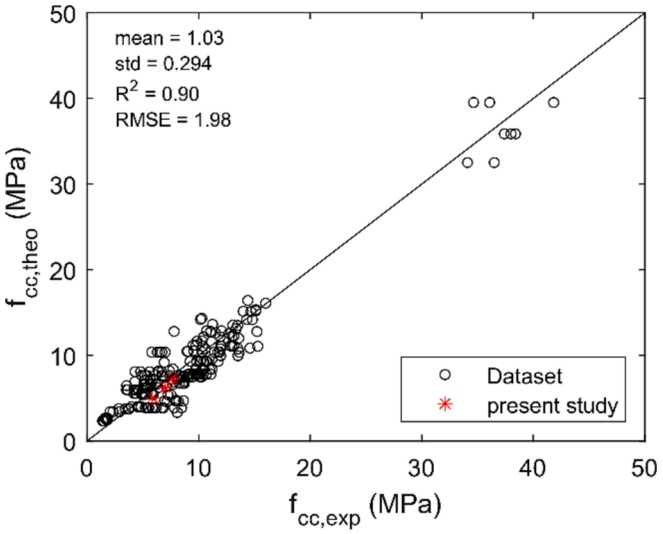

Fig. 7. Assessment of the proposed model for the collected dataset (data in black, circles) and the present experimental campaign (data in red, stars). (For interpretation of the references to colour in this figure legend, the reader is referred to the web version of this article.)

For the unconfined columns, the maximum attained stress depends clearly on the quality of mortar joint, as it is possible to observe from the values of f_{co} shown in Table 6. In fact, the heterogeneity of the experimental f_{c0} follows the differences in the f_j values. As expected, the length of the post-peak curve is higher in the case of the specimens realized with the lower quality mortar. Concerning the results of the confined specimens, instead, the experimental f_{cc} values are less scattered, this depending both on the fact that the same GFRCM system was used for all the columns, and also because there were less differences in the strength of the mortar joint f_j. The results in terms of fiber strains development show that the jacketing system was subject to relevant deformations, being both the peak and ultimate strength corresponding to high strain values. This result indicates a high exploitation ratio of the glass fibers.

The experimental confined strength results are then compared to the predicted ones using the formulation developed in this work (Eq. (11)), and are plotted (in red) together all the other literature results (in black)

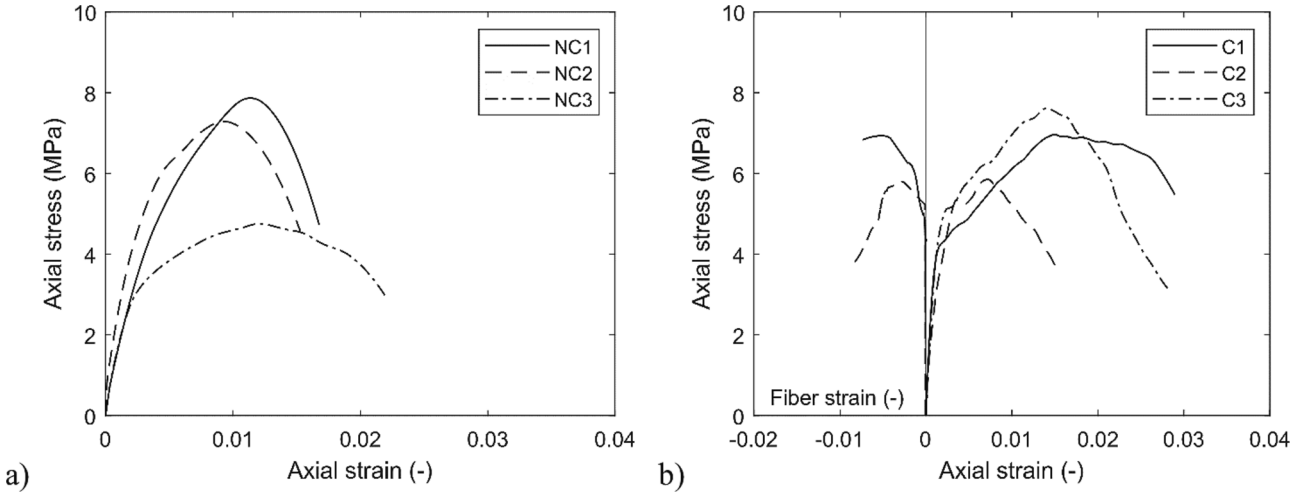

Fig. 6. Stress–strain curves of the: a) NC and b) C columns.

Table 7
Comparison between predicted axial strength values from confinement models.

Model	Columns						
	C1		*C2*		*C3*		Mean error (%)
	$f_{cc,theo}$ (MPa)	$f_{cc,theo}$ / $f_{cc,exp}$	$f_{cc,theo}$ (MPa)	$f_{cc,theo}$ / $f_{cc,exp}$	$f_{cc,theo}$ (MPa)	$f_{cc,theo}$ / $f_{cc,exp}$	
This proposal	**6.27**	**0.90**	**5.07**	**0.87**	**7.31**	**0.96**	**9%**
CNR DT 215 [38]	7.40	1.06	7.42	1.27	7.35	0.97	12%
ACI 549.4R [39]	6.95	1.00	6.95	1.19	6.95	0.91	9%
Cascardi et al. [40]	8.07	1.16	8.26	1.41	7.98	1.05	21%
Jing et al. [20]	8.93	1.28	8.93	1.53	8.93	1.17	33%
Krevaikas - linear [17]	6.62	0.95	6.62	1.13	6.62	0.87	10%
Krevaikas - non linear [17]	6.70	0.96	6.70	1.15	6.70	0.88	10%
Koutas and Bournas [36]	7.33	1.05	7.33	1.25	7.33	0.96	11%
Ameli et al. 1 [22]	6.92	0.99	6.93	1.18	6.91	0.91	9%
Ameli et al. 2 [22]	7.03	1.01	7.04	1.20	7.02	0.92	10%
Napoli and Realfonzo 1 [19]	7.28	1.05	7.28	1.24	7.28	0.96	11%
Napoli and Realfonzo 2 [19]	7.44	1.07	7.44	1.27	7.44	0.98	12%

in Fig. 7. There, the prediction accuracy indicators are listed too, accounting now also for the new results. The new experimental results are well aligned with the predictions, this indicating that the performance of the proposed formulation is high even when accounting for this new set of results. The new *AVE*, R^2, *RMSE* values are almost constant compared to the previous ones obtained on the original dataset. Table 7 compares the predicted axial strength values for the tested columns using the proposed formulation with the confined strength computed using the existing models summarized before in Table 3. The mean error results 9%, which is the lowest between the considered models together with the ACI 549.4R [39] and Ameli et al. 1 [22]. Compared to the new test data, the proposal results slightly conservative with a mean $f_{cc,theo}$ / $f_{cc,exp}$ value of 0.91.

6. Conclusions

Typical formulations for estimating the confined compressive strength of masonry columns are based on best fitting equations calibrated on limited dataset. Furthermore, they generally estimate the confined masonry capacity based on the knowledge of the unconfined compressive strength. However, often in existing masonry structures there is a great heterogeneity of the materials property, which is magnified due to the presence of localized damage in the mortar joints and only seldom in the bricks (clay-based or made with natural stones). To characterize such variability, a large number of in situ tests are required, that are generally destructive or partially destructive, such as in the case of the flat jack tests. Alternatively, non-destructive tests can be carried out to estimate the mortar joint strength only, which can be carried out easily and with a sufficient numerousness, e.g. via penetrometer tests.

Based on this context, in this work a new formulation to predict the confined compressive strength of masonry columns is proposed, that includes directly bricks and mortar joint compressive strength in its formulation. The proposal introduces some novelties also in the calculation of the effective confinement pressure.

The new formulation is calibrated on a wide dataset, showing better accuracy indicators than the others reviewed from the literature. The proposal is also validated on a new set of experimental results, which are presented in this work, and that deal with confined columns with one layer of GFRCM. According to the authors opinion, the new formulation can be used to estimate the confined masonry strength in those cases where a high variability of masonry properties is present in an existing structure, and is difficult to test and characterize each part of the masonry subject to a different damage condition. For instance, the situations can be those where localized phenomena affect the quality of the mortar joints or the bricks separately, e.g., in presence of soluble salts crystallization, carbonation of the mortar and bicarbonation of the stones, exfoliation of the masonry, mechanical damage due to external actions, etc.

CRediT authorship contribution statement

Flora Faleschini: Conceptualization, Methodology, Data curation, Investigation, Resources, Supervision, Project administration. **Klajdi Toska:** Conceptualization, Methodology, Data curation, Investigation, Formal analysis, Visualization.

Declaration of Competing Interest

The authors declare that they have no known competing financial interests or personal relationships that could have appeared to influence the work reported in this paper.

Data availability

The authors confirm that the data supporting the findings of this study are available within the article and its supplementary materials.

Acknowledgments

The authors would like to thank G&P Intech for providing the FRCM system. Also, Eng. Alessia Casarotti and Eng. Lucia Sambataro are kindly acknowledged for their help during the experimental campaign. The work has received fundings from DOR (Dotazione Ordinaria Ricerca) by the University of Padova, ICEA Department.

Appendix A. Supplementary material

Supplementary data to this article can be found online at https://doi.org/10.1016/j.compstruct.2023.117587.

References

[1] De Santis S, de Felice G. Shake table tests on a tuff masonry structure strengthened with composite reinforced mortar. Compos Struct 2021;275:114508.
[2] Minafò G, La Mendola L. Experimental investigation on the effect of mortar grade on the compressive behaviour of FRCM confined masonry columns. Compos B Eng 2018;146:1–12.
[3] Kržan M, Bosiljkov V, Gostič S, Zupančič P. Influence of ageing and deterioration of masonry on load bearing capacity of historical building. In: 15th world conference of earthquake engineering, Lisbon, Portugal, vol. 2428; 2012, September.
[4] Kouris LAS, Triantafillou TC. State-of-the-art on strengthening of masonry structures with textile reinforced mortar (TRM). Constr Build Mater 2018;188:1221–33.
[5] Wang J, Wan C, Zeng Q, Shen L, Malik MA, Yan D. Effect of eccentricity on retrofitting efficiency of basalt textile reinforced concrete on partially damaged masonry columns. Compos Struct 2020;232:111585.

[6] Thamboo J. Performance of masonry columns confined with composites under axial compression: a state-of-the-art review. Constr Build Mater 2021;274:121791.
[7] Pinho FF, Lúcio VJ, Baião MF. Experimental analysis of rubble stone masonry walls strengthened by transverse confinement under compression and compression-shear loadings. Int J Architect Heritage 2018;12(1):91–113.
[8] Estevan L, Baeza FJ, Bru D, Ivorra S. Stone masonry confinement with FRP and FRCM composites. Constr Build Mater 2020;237:117612.
[9] D'Anna J, Amato G, Chen JF, Minafò G, La Mendola L. Effectiveness of BFRP confinement on the compressive behaviour of clay brick masonry cylinders. Compos Struct 2020;249:112558.
[10] Aiello MA, Bencardino F, Cascardi A, D'Antino T, Fagone M, Frana I, et al. Masonry columns confined with fabric reinforced cementitious matrix (FRCM) systems: a round robin test. Constr Build Mater 2021;298:123816.
[11] Fossetti M, Minafò G. Strengthening of masonry columns with BFRCM or with steel wires: an experimental study. Fibers 2016;4(2):15.
[12] Murgo FS, Mazzotti C. Masonry columns strengthened with FRCM system: numerical and experimental evaluation. Constr Build Mater 2019;202:208–22.
[13] Aiello MA, Cascardi A, Ombres L, Verre S. Confinement of masonry columns with the FRCM-system: theoretical and experimental investigation. Infrastructures 2020;5(11):101.
[14] Ombres L, Verre S. Analysis of the behavior of FRCM confined clay brick masonry columns. Fibers 2020;8(2):11.
[15] Cascardi A, Micelli F, Aiello MA. FRCM-confined masonry columns: experimental investigation on the effect of the inorganic matrix properties. Constr Build Mater 2018;186:811–25.
[16] Deng M, Li T, Zhang Y. Compressive performance of masonry columns confined with highly ductile fiber reinforced concrete (HDC). Constr Build Mater 2020;254:119264.
[17] Krevaikas TD. Experimental study on carbon fiber textile reinforced mortar system as a means for confinement of masonry columns. Constr Build Mater 2019;208:723–33.
[18] Santandrea M, Quartarone G, Carloni C, Gu XL. Confinement of masonry columns with steel and basalt FRCM composites. In: Key Engineering Materials, vol. 747. Trans Tech Publications Ltd.; 2017. p. 342–9.
[19] Napoli A, Realfonzo R. Compressive behavior of masonry columns confined with FRCM systems: research overview and analytical proposals. J Compos Constr 2022;26(3):04022019.
[20] Jing L, Yin S, Aslani F. Statistical analysis of the compressive strength of fabric-reinforced cementitious matrix (FRCM)-confined masonry columns. Mater Struct 2021;54(3):1–15.
[21] Cascardi A, Aiello MA, Triantafillou T. Analysis-oriented model for concrete and masonry confined with fiber reinforced mortar. Mater Struct 2017;50(4):1–15.
[22] Ameli Z, D'Antino T, Carloni C. A new predictive model for FRCM-confined columns: a reflection on the composite behavior at peak stress. Constr Build Mater 2022;337:127534.
[23] Yilmaz I, Mezrea PE, Ispir M, Binbir E, Bal IE, Ilki A. External confinement of brick masonry columns with open-grid basalt reinforced mortar. In: Proceedings of the fourth Asia-Pacific conference on FRP in structures (APFIS 2013), Melbourne, Australia; 2013, December. p. 11–3.
[24] Ombres L. Confinement effectiveness in eccentrically loaded masonry columns strengthened by fiber reinforced cementitious matrix (FRCM) jackets. In: Key Engineering Materials, vol. 624. Trans Tech Publications Ltd.; 2015. p. 551–8.
[25] Carloni C, Mazzotti C, Savoia M, Subramaniam KV. Confinement of masonry columns with PBO FRCM composites. In: Key Engineering Materials, Vol. 624. Trans Tech Publications Ltd.; 2015. p. 644–51.
[26] Incerti, A., Vasiliu, A., Ferracuti, B., & Mazzotti, C. (2015, December). Uni-Axial compressive tests on masonry columns confined by FRP and FRCM. In: Proc. of the 12th international symposium on fiber reinforced polymers for reinforced concrete structures & the 5th Asia-pacific conference on fiber reinforced polymers in structures, joint conference, Nanjing, China, 14–16 December 2015.
[27] Maddaloni G, Cascardi A, Balsamo A, Di Ludovico M, Micelli F, Aiello MA, et al. Confinement of full-scale masonry columns with FRCM systems. In: Key engineering materials, vol. 747. Trans Tech Publications Ltd.; 2017. p. 374–81.
[28] Mezrea PE, Yilmaz IA, Ispir M, Binbir E, Bal IE, Ilki A. External jacketing of unreinforced historical masonry piers with open-grid basalt-reinforced mortar. J Compos Constr 2017;21(3):04016110.
[29] Witzany J, Zigler R. Stress state analysis and failure mechanisms of masonry columns reinforced with FRP under concentric compressive load. Polymers 2016;8(5):176.
[30] Sneed LH, Carloni C, Baietti G, Fraioli G. Confinement of clay masonry columns with SRG. In: Key engineering materials, vol. 747. Trans Tech Publications Ltd.; 2017. p. 350–7.
[31] Di Ludovico M, Cascardi A, Balsamo A, Aiello MA. Uniaxial experimental tests on full-scale limestone masonry columns confined with glass and basalt FRCM systems. J Compos Constr 2020;24(5):04020050.
[32] Jing L, Yin S, Aslani F. Experimental investigation on compressive performance of masonry columns confined with textile-reinforced concrete. Constr Build Mater 2021;269:121270.
[33] Sneed LH, Baietti G, Fraioli G, Carloni C. Compressive behavior of brick masonry columns confined with steel-reinforced grout jackets. J Compos Constr 2019;23(5):04019037.
[34] Ombres L, Verre S. Masonry columns strengthened with steel fabric reinforced cementitious matrix (S-FRCM) jackets: experimental and numerical analysis. Measurement 2018;127:238–45.
[35] Li T, Deng M, Dong Z, Zhang Y, Zhang C. Masonry columns confined with glass textile-reinforced high ductile concrete (TRHDC) jacket. Eng Struct 2020;222:111123.
[36] Koutas LN, Bournas DA. Confinement of masonry columns with textile-reinforced mortar jackets. Constr Build Mater 2020;258:120343.
[37] Ombres L, Iorfida A, Verre S. Confinement of masonry columns with PBO and basalt FRCM composites. In: Key engineering materials, Vol. 817. Trans Tech Publications Ltd.; 2019. p. 392–7.
[38] CNR - National Research Council. Guide for the design and construction of externally bonded fibre reinforced inorganic matrix systems for strengthening existing structures (version: June, 2020). CNR-DT215/2018. Rome; 2018.
[39] ACI - American Concrete Institute. Guide to design and construction of externally bonded fabric-reinforced cementitious matrix (FRCM) systems for repair and strengthening concrete and masonry structures. ACI 549.4R-20. Farmington Hills, MI; 2020.
[40] Cascardi A, Longo F, Micelli F, Aiello MA. Compressive strength of confined column with fiber reinforced mortar (FRM): new design-oriented-models. Constr Build Mater 2017;156:387–401.
[41] EN 1992-1-1. Eurocode 2: Design of concrete structures - Part 1-1: General rules and rules for buildings. CEN, Brussels, Belgium; 2004.
[42] Dayaratnam P. Brick and reinforced brick structures. New Delhi: Oxford and IBH; 1987.
[43] Kaushik HB, Rai DC, Jain SK. Stress-strain characteristics of clay brick masonry under uniaxial compression. J Mater Civ Eng 2007;19(9):728–39.
[44] En1996.. Eurocode 6: design of masonry structures. Brussels, Belgium: CEN; 2005.
[45] Toska K, Faleschini F. FRCM-confined concrete: monotonic vs. cyclic axial loading. Compos Struct 2021;268:113931.
[46] Toska K, Faleschini F, Zanini M. Confinement of concrete with FRCM: influence of bond aspects. Constr Build Mater 2023. under review.
[47] Di Ludovico M, Prota A, Manfredi G. Structural upgrade using basalt fibers for concrete confinement. J Compos Constr 2010;14(5):541–52.
[48] Colajanni P, De Domenico F, Recupero A, Spinella N. Concrete columns confined with fibre reinforced cementitious mortars: experimentation and modelling. Constr Build Mater 2014;52:375–84.
[49] Faleschini F, Zanini MA, Hofer L, Pellegrino C. Experimental behavior of reinforced concrete columns confined with carbon-FRCM composites. Constr Build Mater 2020;243:118296.
[50] Toska K, Faleschini F, Zanini MA, Hofer L, Pellegrino C. Repair of severely damaged RC columns through FRCM composites. Constr Build Mater 2021;273:121739.